NASA/TM—2001-210899

Effects of Minor Alloying Additions on the Microstructure, Toughness, and Creep Strength of Directionally Solidified NiAl-31Cr-3Mo

J.D. Whittenberger and S.V. Raj
Glenn Research Center, Cleveland, Ohio

I.E. Locci
Case Western Reserve University, Cleveland, Ohio

J.A. Salem
Glenn Research Center, Cleveland, Ohio

May 2001

The NASA STI Program Office . . . in Profile

Since its founding, NASA has been dedicated to the advancement of aeronautics and space science. The NASA Scientific and Technical Information (STI) Program Office plays a key part in helping NASA maintain this important role.

The NASA STI Program Office is operated by Langley Research Center, the Lead Center for NASA's scientific and technical information. The NASA STI Program Office provides access to the NASA STI Database, the largest collection of aeronautical and space science STI in the world. The Program Office is also NASA's institutional mechanism for disseminating the results of its research and development activities. These results are published by NASA in the NASA STI Report Series, which includes the following report types:

- TECHNICAL PUBLICATION. Reports of completed research or a major significant phase of research that present the results of NASA programs and include extensive data or theoretical analysis. Includes compilations of significant scientific and technical data and information deemed to be of continuing reference value. NASA's counterpart of peer-reviewed formal professional papers but has less stringent limitations on manuscript length and extent of graphic presentations.

- TECHNICAL MEMORANDUM. Scientific and technical findings that are preliminary or of specialized interest, e.g., quick release reports, working papers, and bibliographies that contain minimal annotation. Does not contain extensive analysis.

- CONTRACTOR REPORT. Scientific and technical findings by NASA-sponsored contractors and grantees.

- CONFERENCE PUBLICATION. Collected papers from scientific and technical conferences, symposia, seminars, or other meetings sponsored or cosponsored by NASA.

- SPECIAL PUBLICATION. Scientific, technical, or historical information from NASA programs, projects, and missions, often concerned with subjects having substantial public interest.

- TECHNICAL TRANSLATION. English-language translations of foreign scientific and technical material pertinent to NASA's mission.

Specialized services that complement the STI Program Office's diverse offerings include creating custom thesauri, building customized data bases, organizing and publishing research results . . . even providing videos.

For more information about the NASA STI Program Office, see the following:

- Access the NASA STI Program Home Page at ***http://www.sti.nasa.gov***

- E-mail your question via the Internet to help@sti.nasa.gov

- Fax your question to the NASA Access Help Desk at 301–621–0134

- Telephone the NASA Access Help Desk at 301–621–0390

- Write to:
  NASA Access Help Desk
  NASA Center for AeroSpace Information
  7121 Standard Drive
  Hanover, MD 21076

NASA/TM—2001-210899

Effects of Minor Alloying Additions on the Microstructure, Toughness, and Creep Strength of Directionally Solidified NiAl-31Cr-3Mo

J.D. Whittenberger and S.V. Raj
Glenn Research Center, Cleveland, Ohio

I.E. Locci
Case Western Reserve University, Cleveland, Ohio

J.A. Salem
Glenn Research Center, Cleveland, Ohio

Prepared for the
Third International Symposium on Structural Intermetallics
sponsored by The Minerals, Metals, and Materials Society
Jackson Hole, Wyoming, September 23–25, 2001

National Aeronautics and
Space Administration

Glenn Research Center

May 2001

Available from

NASA Center for Aerospace Information
7121 Standard Drive
Hanover, MD 21076

National Technical Information Service
5285 Port Royal Road
Springfield, VA 22100

Available electronically at http://gltrs.grc.nasa.gov/GLTRS

EFFECTS OF MINOR ALLOYING ADDITIONS ON THE MICROSTRUCTURE, TOUGHNESS AND CREEP STRENGTH OF DIRECTIONALLY SOLIDIFIED NiAl-31Cr-3Mo

J.D. Whittenberger and S.V. Raj
National Aeronatuics and Space Administration
Glenn Research Center
Cleveland, Ohio 44135

I.E. Locci
Case Western Reserve University
Cleveland, Ohio 44135

J.A. Salem
National Aeronatuics and Space Administration
Glenn Research Center
Cleveland, Ohio 44135

SUMMARY

A study of the effects of small (0.25 to 1.0 at%) fifth element additions to the structure and mechanical properties of directionally solidified (DS) NiAl-31Cr-3Mo has been undertaken. Essentially all the additions changed the as-DS'ed microstructure from lamellar eutectic grains to cells and, in some cases, introduced NiAl dendrites and/or third phases. In general the alloying additions did not improve strength or toughness over that possessed by the base composition; only Hf and, perhaps Ti, gave a minor increase in elevated temperature creep resistance. The lack of improvement in creep properties is probably due to inability to precipitation harden NiAl.

INTRODUCTION

The B2 crystal structure intermetallic NiAl has a higher thermal conductivity and melting point along with a lower density and superior oxidation resistance when compared to Ni-based superalloys. However binary NiAl is weak at elevated temperatures and only possesses limited room temperature fracture toughness. Directional solidification (DS) of NiAl based eutectics has shown the ability to incorporate an oriented ductile metallic phase within the NiAl matrix which can improve toughness as well as creep resistance (ref. 1). The quaternary NiAl-(34-x)Cr-xMo $\{0.7 \leq x \leq 6$ at%$\}$ system is of particular interest since the early study by Cline and Walter (ref. 2) demonstrated that such Mo levels will produce alternating α-(Cr,Mo) and NiAl lamellar plates instead of α-Cr fibers in a NiAl matrix. Subsequent testing of NiAl-(34-x)Cr-xMo alloys has demonstrated toughnesses ranging from 17 to 22 MPa•$\sqrt{m}$ combined with a 1300 K–$10^{-7}s^{-1}$ strength of about 100 MPa (refs. 2 to 4).

Since slow directional solidification growth rates are expected to a commercial liability and neither Johnson et al. (refs. 1, 5 and 6) nor Whittenberger et al. (ref. 4) have shown that a well-aligned microstructure was necessary for improved mechanical properties, in-depth studies of the effect of DS rate on the structure and mechanical properties of several NiAl-(34-x)Cr-xMo alloys were initiated at the Glenn Research Center. Accompanying these growth rate studies, an investigation of minor fifth element additions to the base NiAl-31Cr-3Mo alloy was also instituted to determine if additional improvements in behavior could be realized. Such an approach seemed worthwhile because very small alloying additions have been shown to increase elevated temperature strength of binary NiAl: i.e., Fe, Hf, Mn, Mo, Nb, Ta, Ti, and Zr in polycrystalline NiAl (refs. 7 to 9) and Hf, Re Ta, and Ti in single crystalline NiAl (ref. 10).

This paper summarizes the findings of an investigation of small fifth element additions in directionally solidified NiAl-31Cr-3Mo. Eleven elements were selected for investigation; these included Co, Cu, Fe, Hf, Mn, Nb, Re, Si, Ta, Ti, and Zr generally in amounts of 0.25, 0.5 and/or 1.0 at%. Because neither the partitioning into NiAl or Cr nor the site occupancy in NiAl was known for all of the fifth elements, a consistent scheme was followed, where all the alloying additions X replaced an equal amount (x) of Cr for an overall composition of Ni-33Al-(31-x)Cr-3Mo-xX.

EXPERIMENTAL PROCEDURES

Approximately 19 mm diameter by 180 mm long bars of 33Ni-33Al-(31-x)Cr-3Mo-xX for directional solidification were produced by induction melting appropriate charges of pure Al, Cr, Ni, X and Ni-50Mo(wt%) in high purity alumina crucibles under an argon atmosphere and casting into a copper chill mold. After cropping the bars were inserted into high purity, 19.1 mm i.d. alumina open ended tubes for directional solidification in a modified Bridgman apparatus under flowing high purity argon. The as-cast bars were superheated to 1855±15 K through induction heating of a susceptor, where the molten metal temperature was monitored by a Type C W/Re thermocouple in a protective ceramic tube inserted to about the mid-point of the melt. To achieve preferential solidification, the Al_2O_3 tube containing the molten metal was pulled through a hole in a fixed position water-cooled copper baffle. In addition to direct radiation to the copper baffle, the heat dissipation, necessary for solidification, was also achieved through conduction to the water-cooled pull ram; all together, this geometry yielded thermal gradients through the liquid/solid interface of about 8 to 10 K/mm. All directional solidification runs were conducted at 12.7 mm/h which had resulted in large diameter planar eutectic grains in the base Ni-33Al-31Cr-3Mo eutectic (refs. 3 and 4). In general directional solidification of each bar was undertaken for about 8 h to produce aligned regions ~100 mm in length.

Compression specimens, fracture toughness bend bars, and chemical and metallography samples were taken from the aligned region in each DS rod by wire electrodischarge machining (EDM). The compression specimens were 8×4×4 mm with the 8 mm sample length parallel to the growth axis, and they were tested in the as-EDM'ed surface condition. The fracture toughness bars, 50 mm long and 6×3 mm in cross-section, were machined in accordance to the ASTM–399 bend specimen geometries (ref. 11). Prior to toughness testing, the as-cast EDM layers were removed by grinding the flat faces of the specimens on emery paper to a finish of 600 grit.

Strength at elevated temperature was determined by a combination of constant load creep testing in lever arm machines and constant velocity testing in a universal testing machine between 1200 and 1400 K in air. All alloys were initially examined via constant velocity experiments at 1300 K, where the samples were compressed along their length between a fixed solid SiC push bar and one moving at 0.017 to 1.7×10^{-6} mm/s to yield nominal strain rates varying from 2×10^{-3} to $2\times10^{-7}s^{-1}$. The autographically recorded load-time curves were converted to true stresses, strains and strain rates via the offset method in combination with a normalization to the final specimen length and the assumption of constant volume. The more promising alloys were then subjected to additional constant velocity testing at 1200 and 1400 K as well as constant load creep testing. Creep experiments were undertaken in 10:1 and 4:1 lever arm creep test machines, where the time dependent deformation was determined through measurement of the relative positions of the ceramic push bars applying the load to the specimen. All the contraction-time data from creep testing were normalized with respect to the final specimen length and converted into true stresses and strains assuming that the sample volume was constant.

Fracture toughness of selected alloys at room temperature was measured in three-point bending in accordance with ASTM E399 (ref. 11) with one main exception: The precracks were generated by using the bridge indentation technique (ref. 12) instead of cyclic fatigue. The test specimens were loaded at a stroke rate of 0.0033 mm/s on a 24 mm support span. The specimen stability was monitored by a clip gage, as required by E399. Due to the small test specimen size used in this study, the clip gage generated a significant stress intensity factor of ~0.7 MPa•√m. This error was corrected in the final calculation of the fracture toughness.

Chemical analysis to determine both major and minor solute metallic elements (Ni, Al, Cr, Mo, X) in the DS material was performed by an inductively coupled plasma (ICP) technique, while the concentrations of nitrogen and oxygen were determined by an inert gas fusion method, and the carbon level was measured by the combustion extraction method. Light optical techniques were used to conduct detailed metallographic observations on both the longitudinal and transverse polished samples taken from the aligned region of each directionally solidified rod. Additionally mounted samples containing the highest concentration of the fifth elements were examined in a scanning electron microscope (SEM) to determine their partitioning.

RESULTS

Alloy Chemistry

The experimentally measured compositions of all the alloys examined in this study are presented in table I, where the amount of intended fifth element addition is utilized as the alloy identification. In addition to the five elements of prime concern (Al, Ni, Cr, Mo and X), this table lists the measured Si and C contents. These two unintentional impurities were reported in most of the DS alloys, where Si is probably due to initial

induction melting in crucibles which contained a SiO_2 binder. Additionally a few of the materials contained minor amounts of Cu (≤0.02 at%), Fe (0.01 at%, with the exception of 1Mn which had 0.06 at% Fe)) and O (0.01 at%).

Taking each level of fifth element alloying addition as a group, the average composition for the 0.25 at% addition was 32.05Ni-33.94Al-30.70Cr-2.95Mo-0.25X, while the average for the 0.5 at% addition was 32.28Ni-34.47Al-29.75Cr-2.95Mo-0.46X and the average for the 1.0 at% addition was 32.26Ni-34.53Al-29.32Cr-2.91Mo-0.89X. These values illustrate that the Mo content was very close to the desired 3 at%, but the Cr levels were about 0.7 at% lower than intended for the 0.5 and 1.0 at% X additions. The most glaring factor, however, in these average values is the Al-rich nature of DS alloys. While the intention was to cast, DS and test materials with Al/Ni ratios of 1, the Al/Ni ratios reported in table I indicate that this goal was not met for essentially all the alloys. While our previous studies of directionally solidify Ni-33Al-31Cr-3Mo (ref. 4) and Ni-33Al-33 Cr-1Mo (ref. 13) have generally resulted in slightly Al-rich compositions (Al/Ni≤1.06), more than half the alloys in table I have Al/Ni≥1.06.

In terms of the intended fifth element compositions, as a group all three DS alloys containing Re, had levels which were consistently much lower than expected and lower than the amounts found after the other alloying additions (table I). Excluding the Re containing alloys and one outlier {0.25Ti}, the DS materials designed to have 0.25 at% actually ranged from 0.19 to 0.28 at%, while those at the 0.5 at% level varied from 0.39 to 0.54 at% and for the 1 at% additions the range was from 0.74 to 1.16 %. The most extreme variation was found in the 0.25Ti alloy which actually contained 0.48 at% Ti. Since melting/casting and directional solidification of the alloys in this work was a one time attempt for each composition, the variations in fifth element additions are reasonable.

Microstructure of DS'ed alloys

The major features found in the microstructures of the DS'ed 33Ni-33Al-(31-xCr)-3Mo-xX alloys are outlined in table II, and examples of the transverse microstructures are given in figure 1. Although transverse sections of the base NiAl-31Cr-3Mo alloy DS'ed at 12.7 mm/h contained mm diameter, lamellar eutectic grains (refs. 3 and 4), most fifth element additions of 0.25 percent or more resulted in ~100 to ~400 μm diameter, cellular microstructures (figs. 1(a) to (d)). Lamellar eutectic microstructures (fig. 1(e)) were only seen in the alloys with 0.25Co, 0.25 to 1.0Fe and 0.25 to 0.5Mn. Dendrites (fig. 1(f)) were found after alloying with Co, Nb, Si, Ta, and more than 0.25 Fe; surprisingly an addition of 0.25Hf yielded dendrites, but higher amounts (0.5 or 1.0Hf) did not.

At least four different types of lamellar structures were found within the cells (table II) including the radial pattern (fig. 1(a)), which was also found after DS'ing the base Ni-33Al-31Cr-3Mo after DS'ing at 25.4 mm/h or faster (ref. 4), essentially parallel plates (fig. 1(b)), a Nautilus spiral (fig. 1(c)) and a hand fan, shell-like distribution (fig. 1(d)). Of these four configurations only the parallel plate one (fig. 1(b)) is similar to that found in the large grain, lamellar eutectic structure (fig. 1(e)). In addition to morphology and size differences, other major distinction between lamaller eutectic grains and cells is the appearance of intercellular regions where the NiAl and (Cr,Mo) lamella become much coarser than those in the cell interior. This can be seen through comparison of the sharp transition from grain to grain in the 0.5 Mn lamellar eutectic (fig. 1(e)) to the beginning of cell formation in 0.25Cu (fig. 1(a)) where the sharp transition breaks down and the lamella become fewer and thicker at the triple points.

The intercellular regions can become relatively broad and comprise a large fraction of the total structure (fig. 1(d)). Additionally the lamella within the intercellular regions can break down and form globular (Cr, Mo) in the NiAl matrix (table II). Such changes to the intercellular morphology can range from a relatively few precipitates (fig. 1(g)) to significant numbers which dominate the structure between cells (fig. 1(h)).

Results for the fifth element phase partitioning, based on SEM examination of samples with the highest alloying content, are also given in table II. This study indicated that Co, Cu, Fe, Hf, and Ti were concentrated in NiAl, while Nb, Re, Si, Ta and Zr were mostly in (Cr,Mo). While iron appeared in both NiAl and (Cr,Mo), the location of Mn could not be determined due to the overlap in Cr K_β and Mn K_α intensity peaks. Third phases could be formed with Hf, Nb, Ta or Zr additions, where these phases generally appeared in the intercellular regions. The highest concentration of third phase seen in the DS'ed materials occurred in the 1.0 Hf alloy (fig. 1(i)).

Compression Testing

With a few exceptions (1.0Fe, 1.0Nb, 1.0Ta and 0.5Zr), all the DS alloys identified in tables I and II were compression tested at 1300 K, and figure 2 presents two sets of 1300 K stress-strain curves from constant velocity testing and several creep curves from constant load creep testing. The stress-strain plots in parts (a,b) illustrate the typical behavior observed during testing of all the DS'ed alloys: namely at each imposed strain rate (1) flow occurred at more or less constant stress after a small amount of work hardening or (2) initial work hardening was followed by strain softening; additionally these plots show that the strength of each alloy decreases as the deformation rate is deceased. Compressive creep (fig. 2(c)) in the directionally solidified Ni-33Al-(31-x)Cr-3Mo-xX materials was generally normal with well defined first and second stages as demonstrated by the 1300 K–40 MPa curve for 0.25 Nb and the 1300 K–60 MPa curve for 0.5Hf.

The flow stress (σ)–deformation rate ($\dot{\varepsilon}$) behavior of the DS'ed Ni-33Al-(31-x)Cr-3Mo-xX materials was characterized using the stress and strain rate at 1 percent deformation from each constant velocity test (figs. 2(a) and (b)) along with the steady state creep rates and the average true stresses from the constant load creep experiments (fig. 2(c)). Figure 3 illustrates the 1300 K σ–$\dot{\varepsilon}$ properties for 0.25Nb and 0.5Hf and compares them to those for the directionally solidified base Ni-33Al-31Cr-3Mo alloy (refs. 4 and 13), also grown at 12.7 mm/h, where the results from constant velocity testing are designated by open symbols and those from constant load creep testing are shown as filled symbols. As can be visualized in this figure, the flow stress-strain rate properties were not dependent on the test method, and such independence was true for all the compression tested materials.

The 1300 K flow stress-strain rate properties of the DS'ed alloys were characterized by the constant temperature forms of either an exponential law (eq. (1)) or a power law (eq. (2)),

$$\dot{\varepsilon} = A \exp(C\sigma)\exp(-Q/(RT)); \tag{1}$$

$$\dot{\varepsilon} = A\, \sigma^{n}\exp(-Q/(RT)); \tag{2}$$

where A is a constant (s^{-1}), C is the stress constant, Q is the activation energy (kJ/mol), R is the universal gas constant, T is the absolute temperate and n is the stress exponent. The choice of equations (1) or (2) was simply based on their ability to describe the experimental results for the fifth element additions; for example the exponential law, as demonstrated by the solid line in figure 3(a), best characterized the 0.25Nb data, while the solid curve from a power law fit was able to best represent the 0.5Hf behavior (fig. 3(b)). The dashed lines in figure 3, which define the behavior for DS'ed Ni-33Al-31Cr-3Mo, indicated that either an exponential or a power law can be used for the base alloy.

Semi logarithmic plots of the 1300 K flow stress-strain rate properties for the other 24 directionally solidified alloys are presented in figure 4 along with the dashed curve which characterizes the behavior of DS'ed Ni-33Al-31Cr-3Mo. Disappointingly, there are very few data points above the dashed line which would indicate a stronger material. Alloying with Si (fig. 4(a)); 0.5Fe or 0.5Nb (fig 4(b)) in addition to 0.25 Nb (fig. 3(a)); Re (fig. 4(c) or 0.5 Ta (fig. 4(d)) is clearly detrimental. The potential effectiveness of the remaining fifth element additions was tested utilizing linear regression techniques with a dummy variable in conjunction with equations (1) or (2). This analysis revealed that only 0.5Hf (fig. 3(b)) and 1.0Hf (fig. 4(b)) produced a statistically meaningful improvement in 1300 K strength. While Cu (fig. 4(a), 0.25Fe and 0.25Hf (fig. 4(b)), 0.5Mn (fig. 4(c)), or 0.25 to 1.0Ti (fig. 4(d)) do appear to produce a small increase in strength on visual examination; such an enhancement could not be confirmed by the dummy variable test.

For documentation the deformation parameters (A,C or n), standard deviations for stress constant or stress exponent (δ_C, δ_n) and the coefficient of deviation, R_d^2, from linear regression fits to either equations (1) and (2) for all the 1300 K compression tested DS'ed materials are given in table III(a). While two separate DS'ed bars of 0.25Re were compression tested (fig. 4(c)), both possessed statistically identical properties; therefore the data were joined to give the set of deformation parameters in table III(a). Additionally, the far right hand column of this table presents the results from the comparisons of the 1300 K strength behavior of the DS'ed alloys with fifth element additions to that of the DS'ed unmodified base alloy, where the properties of the vast majority of alloys have been unchanged or adversely affected.

While both 0.5 and 1.0Hf additions do improve the 1300 K strength of DS'ed Ni-33Al-31Cr-3Mo (table III), statistical testing with a dummy variable indicated that the flow stress-strain rate properties of both Hf modified alloys were identical. Therefore, for all practical purposes, out of eleven different alloying additions only 0.5 at% Hf resulted in an improvement at 1300 K. Due to this less than encouraging result, only a few alloys were compression tested at 1200 and 1400 K to check the consistency of behavior at lower/higher temperatures. Examples of 1200 to 1400 K flow stress-strain rate properties are given in figure 5 along with the solid curves from regression fits of the data to equation (2) and dashed lines from regression fitting of the

DS'ed base alloy. By eye one can see that elevated temperature behavior of 0.5Cu (fig. 5(a)) is about the same as the base alloy, while 0.5Hf (fig. 5(b)) and 0.25Ti (fig. 5(c)) have somewhat better strength than the base. Increasing the Ti level to 1.0 at% (fig. 5(d)), however, does not provide any addition advantage, and, in fact, the higher Ti level appears to have decrease the properties in comparison to 0.25Ti (fig. 5(c))

Table III(b) presents the deformation parameters and their standard deviations from the temperature compensated power law regression fits for each alloy along with the range of temperature and strain rate utilized in the analysis. The last column in this table gives the results from the dummy variable comparison of the elevated temperature properties of DS'ed fifth element addition alloys to the base Ni-33Al-31Cr-3Mo. As shown only the 0.5Hf (fig. 5(b)) and 0.25Ti (fig. 5(c)) additions provided any strengthening advantage; the other elements either leave the properties unchanged or weakened.

Room Temperature Fracture Toughness

The room temperature fracture toughness of selected DS'ed alloys is presented in table IV. While at least 3 specimens were prepared from each of the listed compositions, difficulties were encountered in some sets during testing which invalidated results; hence only single datum were obtained for 0.25Fe and 1.0Ti, and only two valid results were measured for 0.25Co, 0.5Si and 1.0Si. Comparison of the existing data for fifth element additions to that for the base alloy does not reveal any positive effect for alloying; in fact most of the alloying additions slightly reduce toughness.

DISCUSSION

The fifth element alloying additions undertaken in this effort were directed at an improvement in the high temperature properties of the NiAl phase in the directionally solidified NiAl-(Cr,Mo) alloys as previous studies (refs. 7 to 10) indicated that such strengthening was possible. However, as is shown in table III, the majority of the alloying additions did not help; only 0.5Hf (and presumably 1.0Hf) and 0.25Ti increased the properties. Even in these two cases (figs. 5(b) and (c)) the improvement was not substantial. In general terms there are several possible reasons for the lack of a positive alloying response such as a change in the lamella microstructure, an absence of precipitation hardening in NiAl, and/or a Al-rich NiAl. On the other hand the apparent strengthening observed in 0.5Hf and 0.25Ti could be a result of solid solution and/or precipitation hardening effects in NiAl.

Lack of Improvement

Changes in the Lamella Microstructure.—An elongated, large grain size, planar eutectic microstructure (refs. 3, 4, and 13) was observed after DS'ing Ni-33Al-31Cr-3Mo at 12.7 mm/h, while under the same growth conditions the majority of the fifth element additions resulted in small diameter cells with a variety of lamella patterns (table II). Thus strength differences due to structure could exist; however the investigations of directional solidification growth rate on the 1200 to 1400 K compressive properties of Ni-33Al-31Cr-3Mo (refs. 4, and 13) have shown that small diameter cells with a radial lamella pattern are as strong as a planar eutectic structure. Therefore weakening from a simple change in lamella morphology does not seem likely.

Absence of Precipitation Hardening of NiAl.—Examination of the alloys with fifth element additions only revealed two instances of small third phase precipitates: 0.25Co had ~0.5 μm diameter Cr-rich particles in NiAl and 1.0Ta had a few ~1 μm thick Ta-rich platelets in the (Cr,Mo) phase. Therefore precipitation of a metallic or intermetallic second phase, which strengthens many NiAl-xX alloys (ref. 14), appears to be absent. While our examination only entailed light optical and scanning electron microscope techniques, the absence of visible precipitates was surprising. The mere presence of Cr in these alloys should lead to many precipitates in NiAl since the solubility of Cr in NiAl is very high at elevated temperatures (~15 at% at the eutectic temperature) and decreases rapidly with temperature (~2 percent at 800 K) (ref. 15). It is probable, however, that the combination of a slow DS'ing rate and short diffusion distances {NiAl lamella thickness, O(5 μm), fig. 1} permitted sufficient Cr to diffuse out of NiAl to (Cr,Mo) during cooling. Thus equilibrium could be maintained between these two phases, and the supersaturated solid solution necessary for precipitation never achieved.

In terms of the fifth element modified alloys, table II indicates that Nb, Re, Si, Ta and Zr additions partition to the (Cr,Mo) phase or even form large third phase regions (Nb, Ta and Zr); thus the remaining concentration of these elements within NiAl is insufficient for precipitation of a strengthening phase. On the other hand Hf does partition to NiAl (table II), but it also forms relatively large regions of a third phase (fig. 1(i)).

These areas are probably Ni_2AlHf(9) since SEM energy dispersive techniques reveal high concentrations of Al, Ni and Hf in these regions. Following the same logic as applied to Cr, the absence of a visible population of Ni_2AlHf particles in the DS'ed Hf-modified Ni-33Al-31Cr-3Mo is probably due to a slow solidification rate and short diffusion distances (fig. 1(i)) which prevent the necessary super saturation.

Al-rich NiAl.—The high Al/Ni ratios (table I) in the Ni-33Al-(31-x)Cr-3Mo-xX alloys strongly suggest that the NiAl component of the DS'ed eutectics would be Al-rich and thus be weak at elevated temperature (ref. 16). By itself the Al/Ni ratio can not conclusively indicate that the NiAl is Al-rich due to a number of competing factors: {1} some Ni and Al probably exist in (Cr,Mo) since Yang et al. (ref. 17) determined that the (Cr,Mo) phase in DS'ed Ni-33Al-34Cr-1Mo contained 1.6 wt% Al and 1.0 wt% Ni; {2} the various elements can reside on the Ni lattice sites (Co), the Al-sites (Cr, Hf, Mo, Nb, Ta, Ti, Zr) or either site (Cu, Fe) (ref. 18), and {3} per table II most of the fifth element additions partitioned to (Cr,Mo). While we are not certain about the composition of NiAl in each of the 30 alloys in table I, high Al/Ni (>1.06) in many of the alloys make it probable that most have Al-rich NiAl and, hence, would be weak at elevated temperature. The possible exceptions to an Al-rich NiAl would be 0.25Co, 0.25-1.0Mn, 0.5 and 1.0Re and 0.25Zr; however none of these alloys demonstrated improved 1300 K strength (fig. 4).

Increased Properties

Precipitation Hardening.—While a uniform dispersion of Heusler particles does not exist in the NiAl phase within the DS'ed Hf-modified alloys (fig. 1(i)), a second precipitation strengthening phase might be involved. Transmission electron microscopy (TEM) investigations of strong single crystalline NiAl-Hf alloys (refs. 19 and 20) has shown the presence of copious numbers of very small G-phase ($Ni_{16}Hf_6Si_7$) particles which can strengthen to 1300 K (ref. 21). Since some Si also exists in the Hf-modified alloys (table I), it is possible that submicron $Ni_{16}Hf_6Si_7$ precipitates were formed and they are partially responsible for the improved properties found in 0.5 and 1.0Hf (figs. 3(a), 4(b) and 5(b)). Recently Chen et al. (ref. 22) studied a DS'ed NiAl-28Cr-5.5Mo-0.5Hf eutectic alloy which had been contaminated with Si, and they reported large blocky Heusler phase between cells, similar to that shown in fig. 1(i)), as well as inhomogeneously distributed G-phase particles within NiAl. Thus $Ni_{16}Hf_6Si_7$ strengthening of 0.5 and 1.0Hf (table I) is possible.

Solid Solution Hardening.—Four of the five elements which partition to NiAl (Co, Cu, Fe, and Ti, table II), are incapable of forming precipitates at the current concentrations: (1) neither Co or Fe should be effective because both can form B2 aluminides that are completely miscible in NiAl; (2) the solubility of Cu in NiAl is >10 at% (ref. 23) and (3) the solubility of Ti in NiAl is ~5 at% (ref. 24). Thus the additions of Co, Fe, Cu and Ti could only result in solid solution strengthening of NiAl. Of these four elements, only one Ti-modified alloy (fig. 5(c)) exhibited properties beyond those of the base alloy.

Ti has been shown to be a very effective solid solution elevated temperature strengthening addition to polycrystalline (ref. 25) and single crystalline NiAl single crystals (ref. 10). Therefore it is perfectly reasonable to expect a positive response after noting that Ti partitions to NiAl in DS'ed Ni-33Al-(31-x)Cr-3Mo-xTi (table II). While this is certainly the case for the results presented in figure 5(c)), the actual effectiveness of Ti additions is in doubt. The strong alloy identified 0.25Ti in reality contains almost a half percent Ti (table I), yet it possesses greater 1300 K strength than 0.5Ti which also contains about half a percent Ti (fig. 4(d)). Furthermore the 1200 to 1400 K properties of 1.0Ti (fig. 5(d)) are less than those of 0.25Ti (fig. 5(c)). Such behavior is not consistent with any solid solution concept.

While part of the enhanced strength of the DS'ed 0.5Hf (figs. 3(b), 4(b)) could be the result of $Ni_{16}Hf_6Si$ particles, some of the improvement should be the result of solid solution strengthening of NiAl. In fact Darolia and Walston (ref. 26) concluded that creep strength in complex NiAl-based single crystals alloyed with 0.5Hf-0.05Ga and 1.0 or 5.0Ti at temperatures ≥1255 K was entirely due to Hf and Ti solid solution hardening. Because all known investigations of Hf-modified NiAl have contained Si which lead to the formation of G-Phase, the individual contributions of solid solution strengthening and precipitation hardening mechanisms of Hf are not certain.

Summary of Elevated Temperature Behavior

The most probable cause for the lack of improved elevated temperature strength in the DS'ed fifth element materials is due to the partitioning of the alloying elements to the (Cr,Mo) phase and/or formation of large third phase regions. Both of these tendencies prevented super saturation in NiAl and removed the possibility of fifth element precipitation hardening of NiAl. Based on negligible strengthening, it must also be concluded that the current fifth element additions were insufficient to harden the (Cr,Mo) phase. Two alloying additions

did show some promise, where strengthening due to Hf is probably due to both solid solution and precipitation hardening of NiAl. Although one Ti addition did strengthen, data gathered for the other two Ti-containing alloys was not consistent with an improvement.

Room Temperature Toughness

Only a few of the 31 DS'ed bars containing fifth elements were examined for their room temperature toughness (table IV), and none of these alloys demonstrated any significant improvement over the values from three different determinations for the DS'ed Ni-33Al-31Cr-3Mo base alloy (refs. 4, 13, and 27). In hindsight the 8 alloys tested for toughness were not the best choices based on microstructure (table II) and the current analysis of elevated temperature properties (figs. 3 to 5). However one of the two strongest alloys (0.25Ti) was selected for testing, but no valid samples could be produced. Based on our limited toughness testing, there does not appear to be any advantage to fifth element alloying.

SUMMARY OF RESULTS

A study of the mechanical properties of directionally solidified Ni-33Al-31Cr-3Mo alloyed with small fifth element additions did not demonstrate any significant improvement in elevated temperature strength or room temperature toughness. The inability to increase creep resistance is probably due to the lack of significant precipitation hardening in NiAl.

REFERENCES

1. D.R Johnson, X.F. Chen, B.F. Oliver, R.D. Noebe and J.D.Whittenberger, *Intermetallics* **3** (1995) pp. 99–113.
2. H.E. Cline and J.L. Walter, *Metal. Trans.*, **1** (1970) pp. 2907–2917.
3. S.V. Raj, I.E. Locci and J.D. Whittenberger, Creep Behavior of Advanced Materials for the 21st Century (eds. R.S. Mishra, A.K. Mukherjee and K.L Murty), TMS Warrendale, PA, 1999, pp. 295–310.
4. J.D. Whittenberger, S.V. Raj, I.E. Locci, and J.A. Salem. *Intermetallics* **7** (1999) pp. 1159–1168.
5. D.R. Johnson, X.F. Chen, B.F. Oliver, R.D. Noebe and J.D. Whittenberger, *Intermetallics* **3** (1995) pp. 141–152.
6. D.R. Johnson, B.F. Oliver, R.D. Noebe and J.D.Whittenberger *Intermetallics* **3** (1995) pp. 493–503.
7. K. Vedula, V. Pathare, I. Aslanidis and R.H. Titran, High Temperature Intermetallics Alloys, MRS Proceedings Vol. 39, Pittsburgh, PA 1985, pp. 411–421.
8. R.R. Bowman, R.D. Noebe, S.V. Raj and I.E. Locci, *Metall. Trans. A* **23A** (1992) pp. 1493–1508.
9. C.T. Liu and J.A. Horton, Jr., *Mater. Sci. Eng. A* **192/193** (1995) pp. 170–178.
10. W.S. Walston, R.D. Field, J.R. Dobbs, D.F. Lahrman and R. Darolia, Structural Intermetallics, R. Darolia, J.J. Lewandowski, C.T. Liu, P.L. Martin, D.B. Miracle and M.V. Nathal, eds. (The Minerals, Metals and Materials Society, Warrendale PA, 1993), pp. 523–532.
11. "Standard Test Method for Plane-Strain Fracture Toughness of Metallic Materials." Test Method E 399-90, Annual Book of ASTM Standards, 03.01, ASTM, West Conshohocken, PA, 1990.
12. "Standard Test Method for Fracture Toughness of Advanced Ceramics," Test Method PS070, American Society for Testing Materials Annual Book of ASTM Standards, 15.01 ASTM, West Conshohocken, PA, 1998.
13. S.V. Raj, J.D.Whittenberger, I.E. Locci, and J.A. Salem, unpublished.
14. J.D. Whittenberger, L.J. Westfall and M.V. Nathal. *Scripta Met*. **23** (1989) pp. 2127–30.
15. J.D. Cotton, R.D. Noebe and M.J. Kaufman, Structural Intermetallics, R. Darolia, J.J. Lewandowski, C.T. Liu, P.L. Martin, D.B. Miracle and M.V. Nathal, eds. (The Minerals, Metals & Materials Society, Warrendale PA, 1993), pp. 513–522.
16. J.D. Whittenberger, *J. Mat. Sci.* **22** (1987) pp. 394–402.
17. J.-M. Yang, S.M. Jeng, K. Bain and R.A. Amato, *Acta mater*. **45** (1997) pp. 295–305.
18. G. Bozzolo, R.D. Noebe and F. Honecy, *Intermetallics* 8 (2000) pp. 7–18.
19. R. Darolia and W.S Walston, Structural Intermetallics 1997 (ed. M.V. Nathal, R. Darolia, C.T. Liu, P.L. Martin, D.B. Miracle, R. Wagner and M. Yamaguchi) TMS, Warrendale, PA, 1997 pp. 585–94.

20. J.D. Whittenberger, A. Garg, R.D Noebe, W. Scott Walston, and R. Darolia, Structural Intermetallics 1997 (ed. M.V. Nathal, R. Darolia, C.T. Liu, P.L. Martin, D.B. Miracle, R. Wagner and M. Yamaguchi) TMS, Warrendale, PA, 1997 pp. 631–640.
21. J.D. Whittenberger, I.E. Locci, Ram Darolia, and R. Bowman. *Mater. Sci. Eng. A.* **A268** (1999) pp. 165–83.
22. Y.X Chen, C.Y. Cui, Z.Q. Liu, L.L. He, J.T. Guo and D.X. Li, *J. Mater. Res*. **15** (2000) pp. 1261–70.
23. H. Lipson and A. Taylor, *Proc. Royal Soc*. **A173** (1939) 232.
24. G. Bizzolo, R.D. Noebe, J. Ferrante, and A. Garg, Structural Intermetallics 1997 (ed. M.V. Nathal, R. Darolia, C.T. Liu, P.L. Martin, D.B. Miracle, R. Wagner and M. Yamaguchi) TMS, Warrendale, PA, 1997 pp. 655–64.
25. J.D. Whittenberger, R.K. Viswanadham, S.K. Mannan, and K.S. Kumar, *J. Mat. Res*. **4** (1989) pp. 1164–71.
26. R. Darolia and S. Walston, Structural Intermetallics 1997 (ed. M.V. Nathal, R. Darolia, C.T. Liu, P.L. Martin, D.B. Miracle, R. Wagner and M. Yamaguchi) TMS, Warrendale, PA, 1997 pp. 585–94.
27. I.E. Locci, S.V. Raj, J.D. Whittenberger, J.A. Salem, D.J. Keller, High-Temperature Ordered Intermetallic Alloys VIII, Vol. **552**, (eds. Easo P. George, Michael J. Mills and Masaharu Yamaguchi), Materials Research Society, Pittsburgh, PA, 1999, pp. KK8.1.1–KK8.1.6.

TABLE I.—COMPOSITIONS AND Al/Ni RATIOS IN ALIGNED REGIONS OF THE DS Ni-33Al-(31-x)Cr-3Mo-xX ALLOYS

Intended fifth element alloying addition	Composition, At. %							Al/Ni ratio
	Ni	Al	Cr	Mo	X	Si	C	
0.25Co	32.81	32.18	31.75	2.97	0.25Co		0.04	0.98
0.25Cu	32.11	33.89	30.66	2.87	0.25Cu	0.15	0.06	1.06
0.5 Cu	32.28	34.25	29.86	2.96	0.46Cu	0.12	0.06	1.06
1.0Cu	32.35	34.15	29.47	3.01	0.90Cu	0.08	0.03	1.06
0.25Fe	32.11	34.42	30.03	3.02	0.24Fe	0.13	0.04	1.07
0.5Fe	32.60	35.55	28.30	2.98	0.44Fe	0.08	0.04	1.09
1.0Fe	31.48	33.64	30.66	3.06	1.05Fe	0.09	0.02	1.07
0.25Hf	31.29	35.61	29.95	2.83	0.19Hf	0.04	0.07	1.14
0.5Hf	31.48	34.96	29.90	3.03	0.54Hf	0.02	0.05	1.11
1.0Hf	31.91	35.07	28.91	2.80	1.16Hf	0.05	0.08	1.10
0.25Mn	33.27	32.68	30.81	2.99	0.22Mn		0.02	0.98
0.5Mn	33.18	32.68	30.63	2.98	0.48Mn		0.04	0.98
1.0Mn	32.44	32.84	30.52	3.17	0.94Mn		0.02	1.01
0.25Nb	31.54	35.95	29.36	2.80	0.26Nb	0.05	0.04	1.14
0.5Nb	32.35	35.81	28.27	2.96	0.47Nb		0.12	1.11
1.0Nb	32.02	36.06	27.97	2.99	0.84Nb	0.04	0.07	1.13
0.25Re	31.79	33.80	31.37	2.71	0.15Re	0.09	0.08	1.06
0.5Re	33.40	33.43	30.04	2.61	0.37Re	0.07	0.05	1.00
1.0Re	34.25	35.15	27.36	2.44	0.65Re	0.09	0.05	1.03
0.25Si	34.54	34.74	30.49	2.88	0.28Si		0.06	1.10
0.5Si	31.92	34.90	29.76	2.97	0.40Si		0.04	1.09
1.0Si	32.11	36.13	28.08	2.89	0.74Si		0.05	1.13
0.25Ta	31.19	34.19	31.50	2.78	0.28Ta	0.02	0.03	1.10
0.5Ta	31.33	34.79	30.57	2.89	0.39Ta	0.02	0.02	1.11
1.0Ta	32.09	34.20	29.97	2.95	0.75Ta	0.01	0.03	1.07
0.25Ti	31.36	33.86	31.35	2.90	0.48Ti	0.02	0.03	1.08
0.5Ti	31.71	33.63	31.10	3.01	0.52Ti	0.01	0.02	1.06
1.0Ti	31.71	33.54	30.93	2.84	0.94Ti	0.01	0.02	1.06
0.25Zr	32.83	32.99	30.58	3.32	0.24Zr		0.03	1.00
0.5Zr	32.52	34.68	29.12	3.13	0.49Zr	0.05	0.04	1.07

TABLE II.—DESCRIPTION OF THE TRANSVERSE MICROSTRUCTURE IN ALIGNED REGIONS OF THE DS Ni-33Al-(31-x)Cr-3Mo-xX ALLOYS

Intended fifth element at%	Lamellar eutectic grains	Cells	Approx. cell diameter, mm	Cell pattern	NiAl dendrites	Intercellular regions	Globular NiAl in interdendritic regions	Distribution of fifth element		
								NiAl	(Cr,Mo)	Third phase
0.25Co	Yes				Yes			Yes		
0.25Cu		Yes	350	Radial	No	Triple points				
0.5Cu		Yes	400	Radial	No	Yes				
1.0Cu		Yes	250	Radial	No	Yes	Yes	Yes		
0.25Fe	Yes				No					
0.5Fe	Yes				Yes					
1.0Fe	Yes				Yes			Yes	Yes	
0.25Hf		Yes	200	Radial	Yes	Yes	Yes			
0.5Hf		Yes	250	Radial	No	Yes	Yes			
1.0Hf		Yes	200	Radial	No	Yes	Yes	Yes		Yes
0.25Mn	Yes				No					
0.5Mn	Yes				No					
1.0Mn		Yes	400	Radial	No	Yes		Not distinct		
0.25Nb		Yes	200	Straight	Yes	Yes	Some			
0.5Nb		Yes	100	Straight	Yes	Yes	Yes			
1.0Nb		A few	100	Not distinct	Yes	Yes	Yes		Yes	Yes
0.25Re		Yes	200	Nautilus	No	Not distinct				
0.5Re		Yes	150	Shell	No	Yes	Yes			
1.0Re		Yes	100	Shell	No	Yes	Yes		Yes	
0.25Si	Yes			Straight	Yes					
0.5Si		Yes		Straight	Yes	Yes				
1.0Si		Yes		Straight	Yes	Yes			Yes	
0.25Ta		Yes	300	Straight	Yes	Yes	Yes			
0.5Ta		Yes	200	Straight	Yes	Yes	Yes			
1.0Ta		Yes	150	Straight	Yes	Yes	Yes		Yes	Yes
0.25Ti		Yes	300	Radial	No	Yes				
0.5Ti		Yes	300	Radial	No	Yes				
1.0Ti		Yes	300	Radial	No	Yes	Yes	Yes		
0.25Zr		Yes	100	Shell	No	Yes	Yes			
0.5Zr		Yes	100	Shell	No	Yes	Yes		Yes	Yes

TABLE III.—DEFORMATION PARAMETERS FOR DS'ed Ni-33Al-(31-x)-3Mo-xX ALLOYS AND STRENGTH COMPARISON TO BASE ALLOY

(a) 1300 K Fits

Intended fifth element alloying addition	Power law				Exponential law				Strength comparison to base alloy
	A_o s^{-1}	n	δ_n	R_d^2	A_o s^{-1}	C	δ_C	R_d^2	
Base	4.06E-016	4.56	0.52	0.950	4.26E-009	0.0364	0.0025	0.977	
0.25Co					1.08E-009	0.0559	0.0041	0.973	Same
0.25Cu	1.78E-0.13	3.16	0.39	0.943					Same
0.5Cu					1.33E-009	0.0433	0.0038	0.963	Same
1.0Cu					2.83E-009	0.0465	0.0026	0.985	Weaker
0.25Fe					2.46E-009	0.0419	0.0048	0.938	Same
0.5Fe					3.80E-009	0.0466	0.0038	0.963	Weaker
0.25Hf	4.67E-020	6.42	0.47	0.974					Same
0.5Hf	5.30E-019	5.77	0.27	0.989					Stronger
1.0Hf	1.11E-018	5.66	0.23	0.989					Stronger
0.25Mn					5.30E-008	0.0265	0.0029	0.966	Weaker
0.5Mn					6.75E-009	0.0353	0.0038	0.924	Same
1.0Mn					5.37E-009	0.0384	0.0013	0.997	Same
0.25Nb					1.38E-008	0.0512	0.0020	0.994	Weaker
0.5Nb	6.45E-020	6.94	0.34	0.988					Weaker
0.25Re					2.89E-009	0.0494	0.0020	0.984	Weaker
0.5Re					8.49E-009	0.0766	0.0051	0.987	Weaker
1.0Re					2.20E-008	0.0497	0.0050	0.071	Weaker
0.25Si					3.74E-009	0.0477	0.0022	0.991	Weaker
0.5Si					3.69E-009	0.0483	0.0019	0.992	Weaker
1.0Si					3.97E-009	0.0769	0.0035	0.990	Weaker
0.25Ta					3.72E-009	0.0409	0.0023	0.988	Same
0.5Ta	5.48E-021	7.43	0.42	0.981					Weaker
0.25Ti					4.48E-009	0.033	0.003	0.947	Same
0.5Ti					2.11E-009	0.039	0.004	0.945	Same
1.0Ti					7.04E-009	0.034	0.002	0.980	Same
0.25Zr					4.32E-009	0.0387	0.0018	0.990	Same

TABLE III.—DEFORMATION PARAMETERS FOR DS'ed Ni-33Al-(31-x)-3Mo-xX ALLOYS AND STRENGTH COMPARISON TO BASE ALLOY

(b) Temperature compensated power law fits

Intended fifth element alloying addition	Temperature, K	Strain rate regime, s^{-1}	A_o s^{-1}	n	Q, kJ/mol	δ_n	δ_Q, kJ/mol	R_d^2	Strength comparison to base alloy
Base	1200	10^{-5} to 10^{-7}							
	1300	10^{-4} to 10^{-8}							
	1400	10^{-3} to 10^{-8}	341	4.66	449.5	0.37	57.3	0.940	
0.25Co	1200	10^{-4} to 10^{-8}							
	1300	10^{-3} to 10^{-8}							
	1400	10^{-3} to 10^{-8}	0.20	6.23	451.1	0.40	48.7	0.942	Same
0.5Cu	1200	10^{-5} to 10^{-8}							
	1300	10^{-5} to 10^{-8}							
	1400	10^{-3} to 10^{-8}	46.9	5.44	469.3	0.40	45.6	0.941	Same
0.5Fe	1200	10^{-4} to 10^{-8}							
	1300	10^{-3} to 10^{-8}	9.24×10^{-4}	6.43	399.7	0.56	64.6	0.927	Same
0.5Hf	1200	10^{-4} to 10^{-8}							
	1300	10^{-3} to 10^{-8}							
	1400	10^{-3} to 10^{-7}	5.36×10^{3}	5.42	528.4	0.18	24.1	0.987	Stronger
0.5Mn	1200	10^{-6} to 10^{-9}							
	1300	10^{-4} to 10^{-8}							
	1400	10^{-3} to 10^{-8}	2.44×10^{5}	4.64	527.9	0.43	50.8	0.924	Same
0.5Re	1200	10^{-5} to 10^{-8}							
	1300	10^{-4} to 10^{-9}	10.0	4.77	408.0	0.31	52.0	0.927	Weaker
0.25Ta	1200	10^{-5} to 10^{-9}							
	1300	10^{-4} to 10^{-8}							
	1400	10^{-3} to 10^{-7}	1.41×10^{4}	5.30	522.0	0.42	43.6	0.946	Same
0.25Ti	1200	10^{-6} to 10^{-9}							
	1300	10^{-4} to 10^{-8}							
	1400	10^{-3} to 10^{-7}	6.95×10^{5}	5.11	568.8	0.43	43.9	0.943	Stronger
1.0Ti	1200	10^{-5} to 10^{-9}							
	1300	10^{-4} to 10^{-8}							
	1400	10^{-3} to 10^{-7}	79.0	5.44	479.2	0.33	33.3	0.960	Same

TABLE IV.—ROOM TEMPERATURE FRACTURE TOUGHNESS FOR SEVERAL DIRECTIONALLY SOLIDIFIED Ni-33Al-(31-x)-3Mo-xX ALLOYS

Intended fifth element at %	Average toughness, MPa·√m	Standard deviation MPa·√m
Base [4,13] Ni-32Al-32Cr-2.7Mo [27]	12.1 12.0	2.0 1.7
0.25 Co	10.7	1.0
0.25 Fe	13.9	
0.25 Si 0.5 Si 1.0 Si	11.8 10.7 11.8	0.35 2.2 1.2
0.25 Re	11.9	0.9
0.5 Ti 1.0 Ti	10.1 9.0	0.9
NiAl-31Cr-3Mo [2]	21.8	0.6
NiAl-34Cr [2]	20.4	1.1

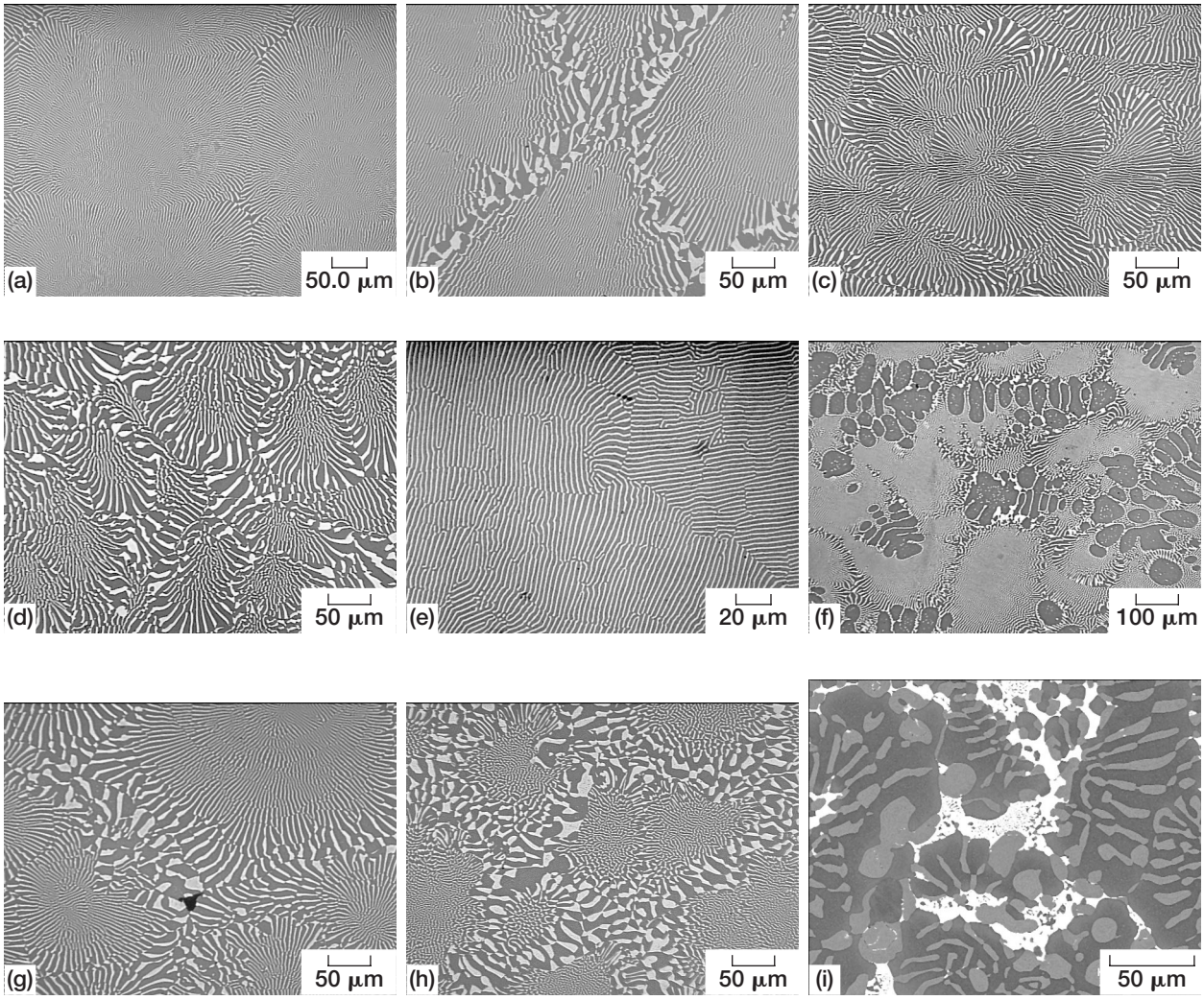

Figure 1.—Light optical (a-h) and scanning electron (i) photomicrographs of the transverse microstructures in the aligned regions of directionally solidified Ni-33Al-(31-x)Cr-3Mo-xX. (a) 0.25 Cu, (b) 0.25Nb, (c) 0.25Re, (d) 1.0Re, (e) 0.5Mn, (f) 1.0Si, (g) 1.0Ti, (h) 1.0Ta and (i) 1.0Hf. In the light optical photomicrographs (a-h) the light contrast phase is (Cr, Mo) and the darker gray phase is NiAl; in the SEM photomicrograph (i) the bright phase in Hf-rich, the gray phase is (Cr, Mo) and the dark phase is NiAl.

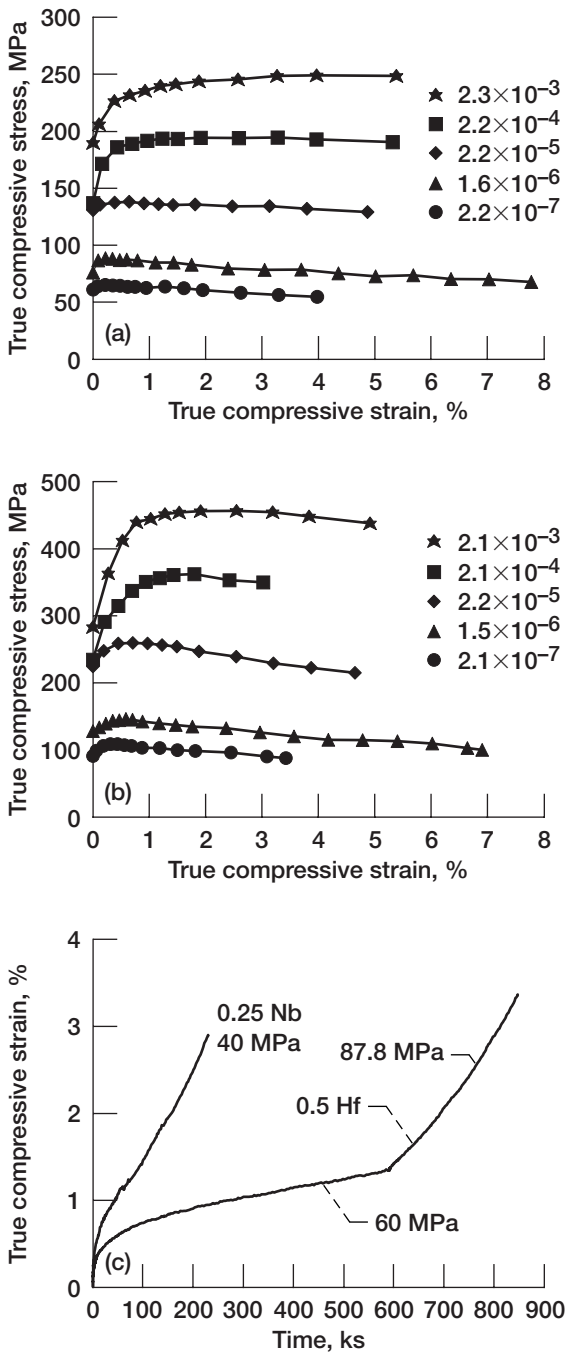

Figure 2.—True 1300 K compressive stress-strain curves as a function of nominal strain rate for directionally solidified Ni-33Al-(31-x)Cr-3Mo-xX alloyed with 0.25Nb (a) and 0.5Hf (b) and true compressive creep curves DS'ed materials containing 0.25Nb and 0.5Hf (c).

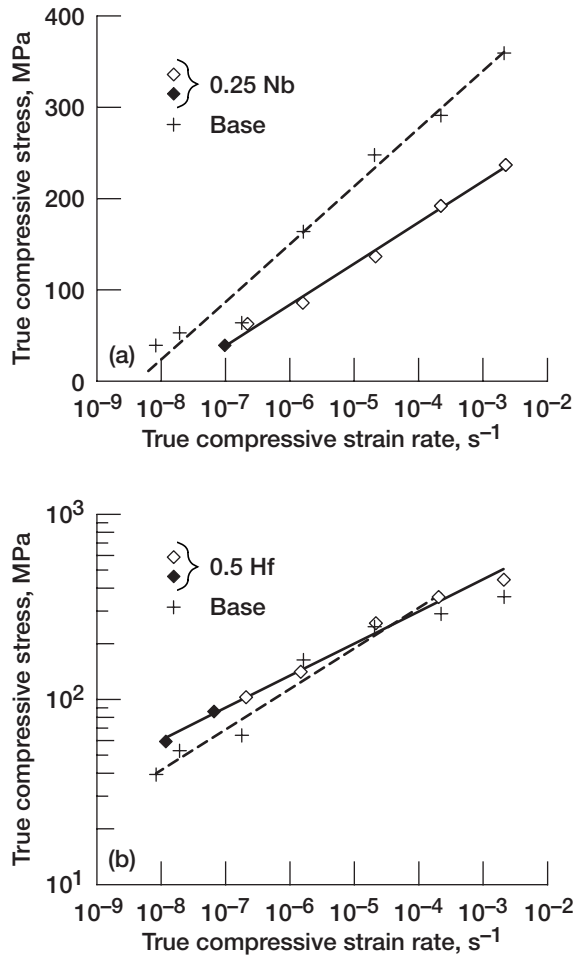

Figure 3.—True 1300 K compressive flow stress-strain rate behavior for directionally solidified Ni-33Al-31Cr-3Mo grown at 12.7 mm/h compared to that for Ni-33Al-(31-x)Cr-3Mo-xX alloyed with (a) 0.25Nb and (b) 0.5Hf.

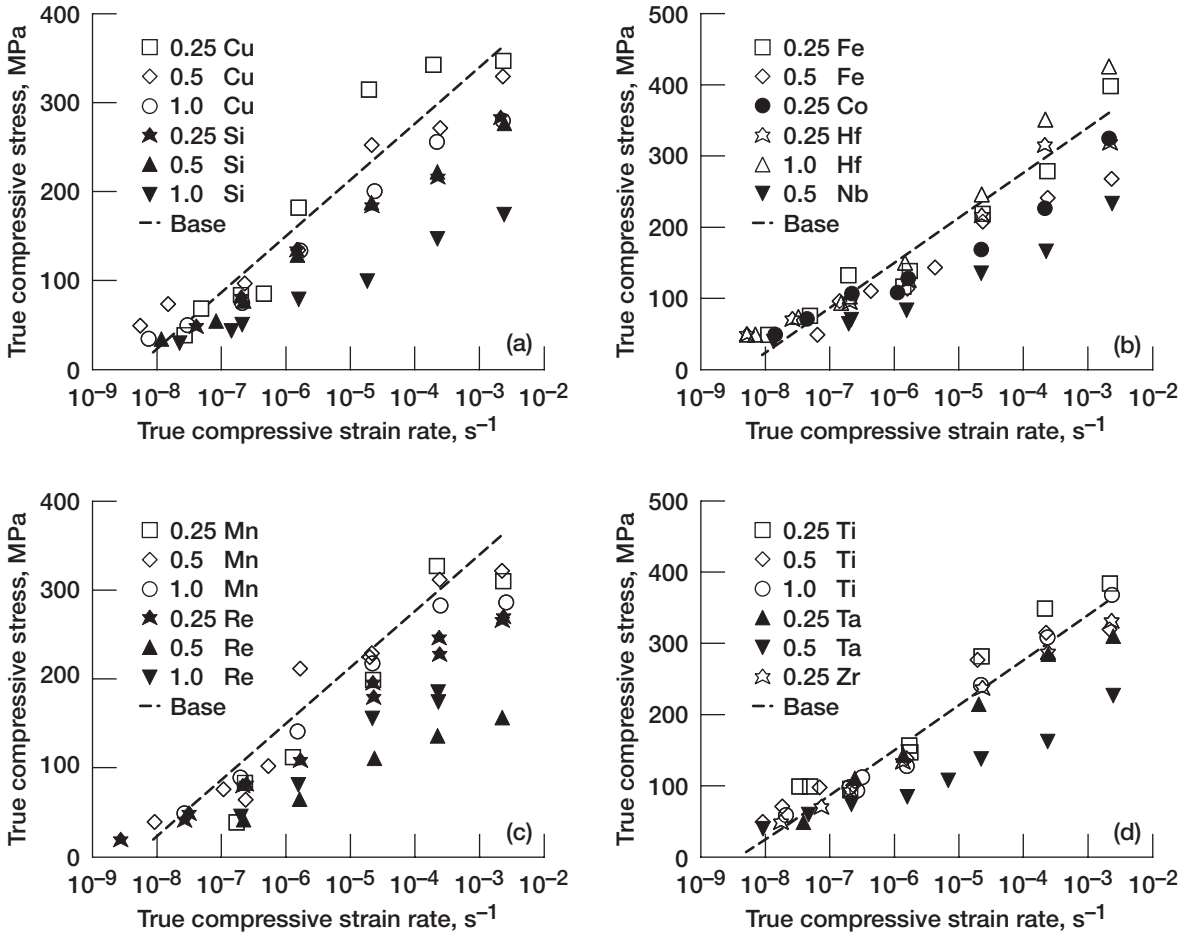

Figure 4.—True 1300 K compressive flow stress-strain rate behavior for directionally solidified Ni33-Al-31Cr-3Mo grown at 12.7 mm/h compared to Ni-33Al-(31-x)Cr-3Mo-xX alloys, where the fifth element additions are (a) 0.25-1.0Cu, 0.25-1.0Si; (b) 0.25Co, 0.25 & 0.5Fe, 0.25 & 1.0Hf, 0.5Nb; (c) 0.25-1.0Mn, 0.25-1.0Re; and (d) 0.25-1.0Ti. 0.25 & 1.0Ta, 0.25Zr. Behavior of the base alloy denoted by the dashed line.

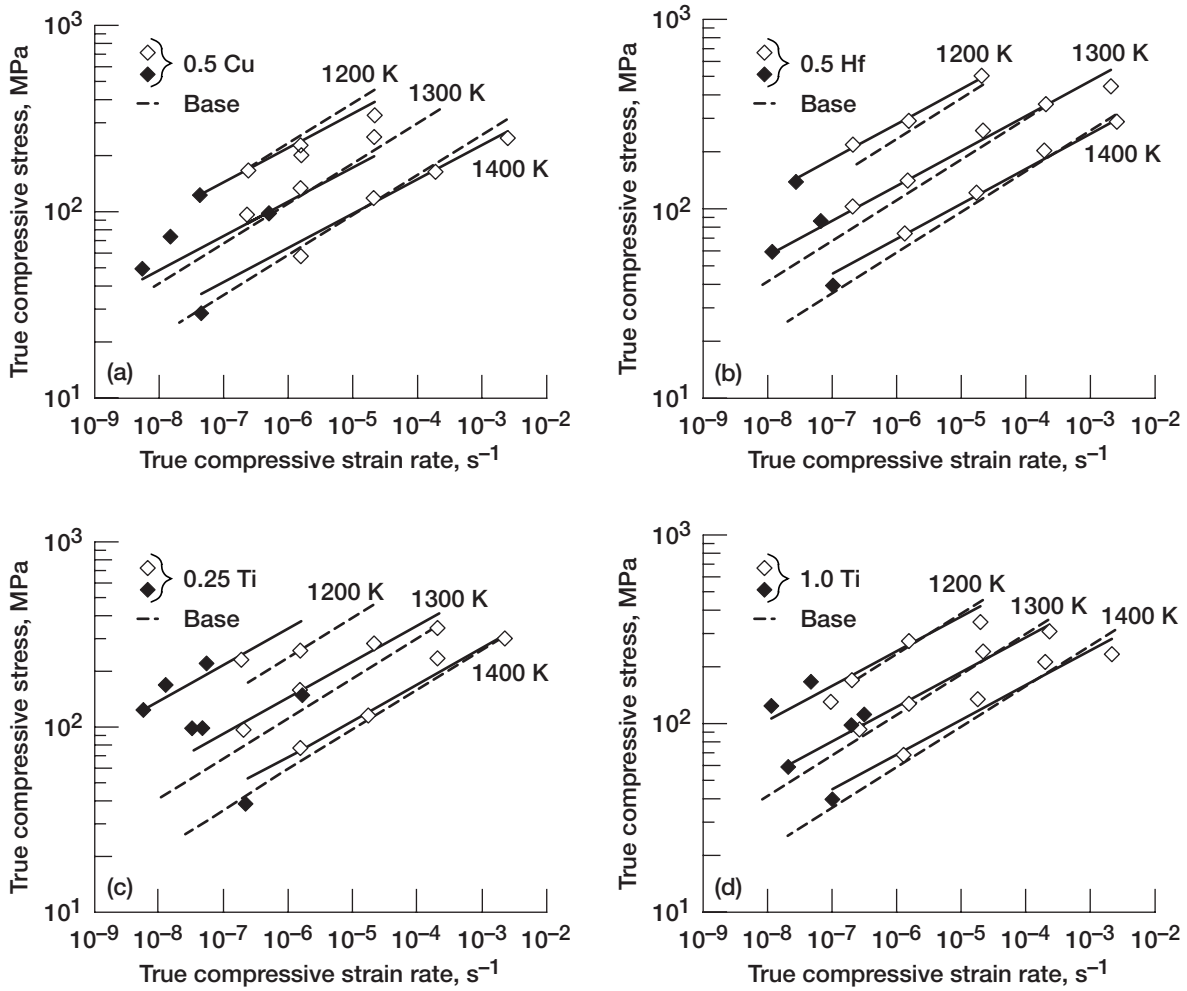

Figure 5.—True 1200-1400 K compressive flow stress-strain rate behavior for directionally solidified Ni-33Al-31Cr-3Mo grown at 12.7 mm/h compared to (a) 0.5Cu, (b) 0.5Hf, (c) 0.25Ti. The open symbols represent data from constant velocity testing, while the filled symbols indicate constant load creep results.

REPORT DOCUMENTATION PAGE

Form Approved
OMB No. 0704-0188

1. AGENCY USE ONLY (*Leave blank*)

2. REPORT DATE
May 2001

3. REPORT TYPE AND DATES COVERED
Technical Memorandum

4. TITLE AND SUBTITLE
Effects of Minor Alloying Additions on the Microstructure, Toughness, and Creep Strength of Directionally Solidified NiAl-31Cr-3Mo

5. FUNDING NUMBERS
WU–708–31–13–00

6. AUTHOR(S)
J.D. Whittenberger, S.V. Raj, I.E. Locci, and J.A. Salem

7. PERFORMING ORGANIZATION NAME(S) AND ADDRESS(ES)
National Aeronautics and Space Administration
John H. Glenn Research Center at Lewis Field
Cleveland, Ohio 44135–3191

8. PERFORMING ORGANIZATION REPORT NUMBER
E–12674

9. SPONSORING/MONITORING AGENCY NAME(S) AND ADDRESS(ES)
National Aeronautics and Space Administration
Washington, DC 20546–0001

10. SPONSORING/MONITORING AGENCY REPORT NUMBER
NASA TM—2001-210899

11. SUPPLEMENTARY NOTES
Prepared for the Third International Symposium on Structural Intermetallics sponsored by The Minerals, Metals, and Materials Society, Jackson Hole, Wyoming, September 23–25, 2001. J.D. Whittenberger, S.V. Raj, and J.A. Salem, NASA Glenn Research Center; I.E. Locci, Case Western Reserve University, Cleveland, Ohio 44106. Responsible person, J.D. Whittenberger, organization code 5120, 216–433–3196.

12a. DISTRIBUTION/AVAILABILITY STATEMENT
Unclassified - Unlimited
Subject Category: 26 Distribution: Nonstandard
Available electronically at http://gltrs.grc.nasa.gov/GLTRS
This publication is available from the NASA Center for AeroSpace Information, 301–621–0390.

12b. DISTRIBUTION CODE

13. ABSTRACT ***(Maximum 200 words)***
A study of the effects of small (0.25 to 1.0 at%) fifth element additions to the structure and mechanical properties of directionally solidified (DS) NiAl-31Cr-3Mo has been undertaken. Essentially all the additions changed the as-DS'ed microstructure from lamellar eutectic grains to cells and, in some cases, introduced NiAl dendrites and/or third phases. In general the alloying additions did not improve strength or toughness over that possessed by the base composition; only Hf and, perhaps Ti, gave a minor increase in elevated temperature creep resistance. The lack of improvement in creep properties is probably due to inability to precipitation harden NiAl.

14. SUBJECT TERMS
NiAl; Cr; Mechanical properties; Intermetallics; Creep; Toughness

15. NUMBER OF PAGES
23

16. PRICE CODE

17. SECURITY CLASSIFICATION OF REPORT	18. SECURITY CLASSIFICATION OF THIS PAGE	19. SECURITY CLASSIFICATION OF ABSTRACT	20. LIMITATION OF ABSTRACT
Unclassified	Unclassified	Unclassified	